Location of the Epidermal Growth Factor Binding Site on the EGF Receptor. A Resonance Energy Transfer Study†

Kermit L. Carraway III, John G. Koland, and Richard A. Cerione*

Department of Biochemistry, Cell and Molecular Biology and Department of Pharmacology, Schurman Hall, Cornell University, Ithaca, New York 14853-6401

Received February 26, 1990; Revised Manuscript Received June 4, 1990

ABSTRACT: As a first step toward developing a structural map of key sites on the epidermal growth factor (EGF) receptor, we have used resonance energy transfer to measure the distance of closest approach between the receptor-bound growth factor molecule and lipid molecules at the surface of the plasma membrane. EGF, specifically labeled at its amino terminus with fluorescein 5-isothiocyanate, was used as an energy donor in these experiments, while either octadecylrhodamine B or octadecylrhodamine 101, inserted into plasma membranes isolated from human epidermoid carcinoma (A431) cells, served as the energy acceptors. The energy transfer measurements indicate that the amino terminus of the bound growth factor is about 67 Å away from the plasma membrane. On the basis of the dimensions of the EGF molecule, this suggests that EGF binds to a site on its receptor that is a considerable distance (52–82 Å) from the surface of these cells. Identical results were obtained under conditions where the receptor functions as an active tyrosine kinase, suggesting that the relative juxtaposition of the EGF binding domain to the membrane surface does not change with receptor autophosphorylation or with the activation of the receptor tyrosine kinase activity.

Epidermal growth factor is a small (M_r = 6040) polypeptide hormone that stimulates cell proliferation in a number of tissues. The binding of EGF[1] to its cell surface receptor triggers the immediate activation of a receptor-associated tyrosine kinase activity (Carpenter, 1987; Hunter & Cooper, 1985; Schlessinger, 1986), which is believed to be crucial in the stimulation of the early and late cellular responses to the growth factor (Chen et al., 1987; Honneger et al., 1988). The receptor for EGF is a 170-kD glycoprotein consisting of at least three separate domains: an extracellular growth factor binding domain, an intracellular tyrosine kinase domain, and a single transmembrane helix connecting the extracellular and intracellular domains (Ullrich et al., 1984).

A key question concerns the mechanisms by which growth factor binding to its receptor at the cell surface transmits a signal across the plasma membrane, culminating in the transduction of the signal to the nucleus. While the receptor tyrosine kinase activity is felt to be an essential component of the mitogenic signaling event, the molecular mechanism by which EGF binding stimulates the tyrosine kinase activity is still poorly understood. Two types of mechanisms have been proposed to explain the EGF-stimulated receptor kinase activity. The first model suggests that EGF-stimulated receptor aggregation is responsible for the activation of the kinase activity (Yarden & Schlessinger, 1987a,b; Boni-Schnetzler & Pilch, 1987). In this intermolecular model, the underlying suggestion is that growth factor binding to the receptor causes conformational changes within the extracellular domain that directly promote the aggregation event. The alternative model suggests that growth factor binding to the extracellular domain causes an intramolecular conformational change that is propagated to the tyrosine kinase active site and elicits a stimulation of the kinase activity (Koland & Cerione, 1988). Growth factor induced conformational changes are key features of both models. In fact, it has recently been demonstrated that EGF binding elicits conformational changes within the extracellular domain of the receptor (Greenfield et al., 1989). However, it has also been shown that divalent cations (Mg^{2+} and Mn^{2+}) induce conformational changes within the receptor tyrosine kinase domain that appear to play a role in regulating the kinase activity and promoting aggregation of the receptor (Koland & Cerione, 1990; Carraway et al., 1989).

An understanding of the relative juxtaposition of key sites within the extracellular and intracellular domains of the EGF receptor will be prerequisite to obtaining insight into the molecular mechanisms underlying the activation and regulation of the EGF receptor tyrosine kinase activity. At the present time, relatively little is known about the details of the tertiary structure of the EGF receptor in solution. We have begun to employ fluorescence approaches to examine the solution structure of the EGF receptor molecule, with the aim of characterizing the relative spatial orientation of key regions on the receptor, as well as the conformational changes accompanying the activation of its kinase activity. In the present study, we have employed resonance energy transfer approaches to determine the location of the receptor-bound EGF molecule relative to the plasma membrane and to determine whether or not the transverse orientation of the bound growth factor molecule changes upon activation of the tyrosine kinase activity.

Experimental Procedures

Materials. Fluorescein 5-isothiocyanate (FITC), octadecylrhodamine B (ORB), octadecylrhodamine 101 (OR101), and [(hexadecyl)amino]fluorescein (HAF) were purchased from Molecular Probes, Inc. Purified murine EGF was the generous gift of Drs. H. A. Scheraga and A. W. Burgess.

† This research was supported by grants from the National Institutes of Health (GM40654), the Pew Biomedical Research Scholars Program, and the Cornell Biotechnology Program, which is supported by the New York State Science and Technology Foundation, a consortium of industries, and the United States Army.

[1] Abbreviations: EGF, murine epidermal growth factor; FITC, fluorescein 5-isothiocyanate; ORB, octadecylrhodamine B, OR101, octadecylrhodamine 101; HAF, [(hexadecyl)amino]fluorescein; FITC-EGF, EGF labeled at its amino terminus with FITC; BSA, bovine serum albumin; DMF, *N*,*N*-dimethylformamide; ex, excitation wavelength; em, emission wavelength.

0006-2960/90/0429-8741$02.50/0

Synthesis of FITC-EGF. Epidermal growth factor was labeled at its amino terminus with FITC and purified as previously described (Carraway et al., 1989). Briefly, EGF was incubated with a 50-fold excess of FITC for 2 h at room temperature in the dark. Protein was separated from unreacted probe with a Sephadex G-10 column. The FITC-EGF adduct was separated from unlabeled growth factor by using a DEAE-Sephacel column eluted with a linear 0–1 M NaCl gradient followed by a 1 M NaCl wash. The stoichiometry of growth factor labeling was estimated to be 1.1 ± 0.1 FITC moieties/EGF molecule, based on extinction coefficients of 19 000 M^{-1} cm^{-1} (278 nm) for EGF (G. Montelione, personal communication) and 75 000 M^{-1} cm^{-1} (495 nm) for FITC.

Cells and Membranes. Human epidermoid carcinoma (A431) cells were grown in Dulbecco's modified Eagle's medium supplemented with 10% fetal calf serum. Plasma membranes from these cells were prepared by a modification of the procedure of Thom et al. (1977) as previously described (Carraway et al., 1989). EGF receptors in the isolated plasma membranes were examined for their ability to bind ^{125}I-EGF and to undergo growth factor stimulated autophosphorylation (Carraway et al., 1989). It was found that ^{125}I-EGF bound to a single class of receptor sites in the plasma membranes with a dissociation constant of 1–2 nM. EGF stimulated the receptor autophosphorylation reaction by as much as 25-fold, yielding a stoichiometry of 3 mol of $^{32}P_i$/mol of ^{125}I-EGF binding sites. Moreover, EGF stimulated the phosphorylation of a synthetic substrate [poly(Glu,Tyr), 4:1; average M_r = 36 000] by membrane receptors,[2] indicating that both the extracellular and intracellular domains of the receptor are accessible to large molecules in intact membranes. Thus, on the basis of a number of criteria, we concluded that the EGF receptors are fully functional within the isolated A431 membranes.

Characterization of FITC-EGF Interactions with Membrane-Bound Receptors. The biological activity of EGF labeled with FITC at its amino terminus was determined by its ability to compete with ^{125}I-labeled EGF for membrane receptors and its ability to stimulate receptor autophosphorylation (Carraway et al., 1989). It was found from the competition studies that FITC-EGF bound to a single class of membrane receptor sites, with a dissociation constant of about 2.5 nM. In addition, FITC-EGF was fully active in its ability to stimulate EGF receptor autophosphorylation. These results indicated that the fluorescein-labeled EGF molecules possessed normal biological activity and should appropriately mimic the native growth factor in structure/function studies. The quantum yield of FITC-EGF was determined to be 0.48 ± 0.02 by comparison with sodium fluorescein in 0.1 N NaOH (Q = 0.92; Weber & Teale, 1957).

Labeling of A431 Cell Plasma Membranes with Fluorescent Amphipathic Probes and Acceptor Density Determination. Octadecylrhodamine B and octadecylrhodamine 101, the two amphipathic probes used as resonance energy transfer acceptors in these experiments, were individually inserted into A431 cell plasma membranes as follows. Aliquots of membranes (5.0 pmol of receptor sites) were suspended in 200 μL of 20 mM Na-HEPES buffer, pH 7.4. Two microliters of either ORB or OR101 in DMF was added to each membrane aliquot such that the added concentration of lipophilic probe was varied from 0 to 36 μM. These incubations were performed in the dark at room temperature for 30 min to allow insertion of the probes into the plasma membranes. Following these incubations, the samples were centrifuged in an Eppendorf microfuge for 10 min to separate labeled membranes from acceptor probes that were free in solution. The membrane pellets were then resuspended in 250 μL of 20 mM HEPES buffer, pH 7.4, containing 0.1 mg of BSA/mL (HB), and the absorption spectrum (450–700 nm) was measured. The concentration of the probes in the resuspended plasma membranes was determined by using the extinction coefficients measured for each probe following its reconstitution into phosphatidylcholine vesicles: 97 300 M^{-1} cm^{-1} (562 nm) for ORB and 67 800 M^{-1} cm^{-1} (586 nm) for OR101.

The density of acceptor probe inserted into the A431 plasma membranes was determined by measuring the energy transfer between donor- and acceptor-labeled lipids as a function of the concentration of acceptor lipid in the membranes. Aliquots of the membranes (125 μL) labeled with various densities of acceptor probe were incubated with either 100 nM or 1.0 μM donor lipid [(hexadecyl)amino]fluorescein (HAF) for 30 min at room temperature. These membranes were then centrifuged to remove unbound HAF and resuspended in 125 μL of HB, and their fluorescence (ex 460 nm, em 518 nm) was determined. The fluorescence values were plotted against the acceptor probe concentration and fit to the function described by Wolber and Hudson for energy transfer in two dimensions, for the case where the distance of closest approach between donor and acceptor lipids is negligible relative to the distance yielding half-maximal energy transfer (Wolber & Hudson, 1979; Holowka & Baird, 1983):

$$Q_{DA}/Q_D = 0.6463 \exp(-4.7497PC) + 0.3537 \exp(-2.0618PC) \quad (1)$$

where C is the micromolar concentration of the acceptor probe in the membrane suspension and P is a variable factor allowing the conversion of acceptor concentration to acceptor density. Each acceptor concentration was multiplied by P to obtain the acceptor density in units of number of acceptor molecules/R_0^2.

Fluorescence Measurements and Energy Transfer Experiments. Fluorescence measurements were made with an SLM 8000 spectrofluorometer operated in the photon counting mode. Samples were held in 0.3-cm quartz cuvettes thermostated at 23 °C. Steady-state anisotropy was determined by

$$A = [(I_v/I_h)/G - 1]/[(I_v/I_h)/G + 2] \quad (2)$$

where (I_v/I_h) is the ratio of the vertical and horizontal emission intensities when the excitation polarizer is in the vertical position and G is the same ratio when the excitation light is horizontally polarized. Anisotropy measurements were made at wavelengths of maximal excitation and emission for each of the probes used in these studies.

In all energy transfer experiments, the fluorescein donor was excited at 460 nm and its emission monitored at 518 nm. The efficiency of energy transfer was measured as the quenching of donor emission and was calculated as

$$E = 1 - Q_{DA}/Q_D \quad (3)$$

where Q_D and Q_{DA} are the quantum yields of the donor in the absence and presence of acceptor, respectively. The value for R_0, which represents the distance (in angstroms) at which the efficiency of energy transfer is 50%, was calculated by

$$R_0 = (9.79 \times 10^3)(J\kappa^2 Q_D n^{-4})^{1/6} \quad (4)$$

where J (in cm^3 M^{-1}) is an integral representing the overlap of donor emission and acceptor absorption, κ^2 is a factor accounting for the respective orientation of donor and acceptor transition dipoles, and n is the refractive index of the medium (Forster, 1959). In our calculations it was assumed that the

[2] K. L. Carraway and R. A. Cerione, unpublished observations.

donor and acceptor dipoles rotate rapidly relative to the fluorescence lifetime of the donor ($\kappa^2 = {}^2/_3$; see Discussion) and that the refractive index of the medium is that of water (1.4). The overlap integrals were calculated as described by Cantley and Hammes (1975).

Experiments to determine the distance of closest approach between FITC-EGF and amphipathic acceptor molecules were designed as titrations of the donor-labeled growth factor into A431 membranes that were labeled to different densities with the acceptor probes. Specifically, eight aliquots (125 μL) of membranes containing 20 nM receptor sites and 0–1.0 acceptor lipids/R_0^2 were prepared for each of the two acceptor lipids. Each of these aliquots was titrated with FITC-EGF in five small aliquots over a range of 0–22 nM, and the fluorescence at 518 nm was recorded. The fluorescence values obtained after each addition were corrected for background and inner filter quenching and plotted as a function of added FITC-EGF concentration.

In the titration experiments described above, some of the FITC-EGF was free in solution (not bound to the membrane receptors). Corrections for the contribution of free growth factor to the overall fluorescence signal were determined by using the equation

$$I_B = F_B L_B = I_T - F_F L_F \quad (5)$$

where I_B is the contribution of the receptor-bound form of the labeled growth factor to the total fluorescence intensity I_T, L_F and L_B are the concentrations of free and receptor-bound FITC-EGF, and F_F and F_B are the fluorescence intensities per unit concentration of the free and bound growth factor. L_F and L_B were calculated on the basis of a model in which FITC-EGF binds to a single class of receptor sites in the plasma membrane:

$$L_F = L_T - \tfrac{1}{2}\{(R_T + L_T + K_D) - [(R_T + L_T + K_D)^2 - 4R_T L_T]^{1/2}\} \quad (6)$$

where R_T and L_T are the total receptor and total ligand (FITC-EGF) concentrations and K_D is the dissociation constant for the interaction of FITC-EGF with the EGF receptor. The concentration of unbound labeled growth factor in these experiments was usually less than 30% of the total. After correction for the contribution of unbound FITC-EGF to the total fluorescence, the efficiency of energy transfer was calculated from the difference between the FITC-EGF fluorescence (F_B from eq 5) observed with unlabeled membranes and the fluorescence observed with membranes labeled with lipophilic acceptor probes. At each acceptor density, five aliquots of FITC-EGF were added to acceptor-labeled membranes, and it was observed that the level of energy transfer between bound FITC-EGF and acceptor lipids was independent of the concentration of the donor molecule in solution. Hence, the energy transfer efficiencies measured with each addition were averaged and plotted against the density of acceptor probe in the plasma membrane. In all, 35 determinations of the distance of closest approach were obtained for each of the two acceptor lipid probes used.

Calculation of the Distance of Closest Approach. The distance of closest approach (L) between FITC-EGF and acceptor lipids in the plasma membrane was obtained by fitting the quenching data to theoretical curves derived from Monte Carlo calculations, as described by Snyder and Freire (1982). For a single donor situated above a plane of acceptors, the energy transfer may be predicted by

$$Q_{DA}/Q_D = [1 + \sum_{i=1}^{N}(R_0/R_i)^6]^{-1} \quad (7)$$

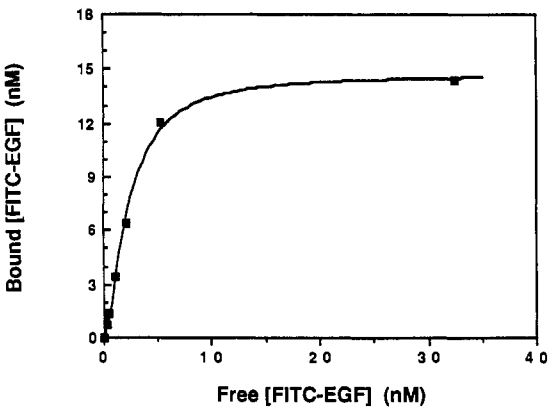

FIGURE 1: Binding of FITC-EGF to A431 plasma membrane receptors. Plasma membranes containing 11 nM ^{125}I-EGF binding sites were incubated with increasing concentrations of FITC-EGF, in the presence and absence of an excess (440 nM) of unlabeled EGF. FITC-EGF/receptor complexes were isolated by centrifugation, and the amount of fluorescence (ex 460 nm, em 518 nm) associated with the pellet and the supernatant was determined. The fluorescence values were converted to FITC-EGF concentrations, and the specifically bound [FITC-EGF] was plotted versus free [FITC-EGF]. The curve through the data points represents the nonlinear least-squares fit to a single class of sites.

where N_A is the total number of acceptors and R_i is the distance to the ith acceptor. This model assumes that the acceptors are randomly distributed in the plane of the membrane. On the basis of this equation, a family of theoretical curves of Q_{DA}/Q_D versus the number of acceptors/R_0^2 were generated for values of L/R_0 ranging from 0.0 to 1.5. Each curve consisted of 11 data points spanning the range of 0.0–1.0 acceptors/R_0^2. The theoretical data points generated by the Monte Carlo calculations were fit to single exponentials (with determined decay constants), and plotted with the experimental quenching data (Figure 6). This single exponential approximation is valid for values of L/R_0 greater than 1.0 and acceptor densities greater than $0.2/R_0^2$, the range in which the experimental data falls. The experimental data for each acceptor lipid were also fit to single exponentials and the decay constants interpolated from the decay constants of the theoretical curves to estimate the values of L/R_0.

Results

Binding of FITC-EGF to A431 Plasma Membranes. We have previously demonstrated that FITC-EGF competes with ^{125}I-EGF for receptor binding sites in isolated plasma membranes with a dissociation constant of about 2.5 nM (Carraway et al., 1989). Figure 1 shows that the interaction of FITC-EGF with the EGF receptor can be monitored by the fluorescence of the growth factor. After incubation with increasing concentrations of the labeled growth factor, the membrane/FITC-EGF complexes were isolated by centrifugation and resuspended, and the fluorescence was determined. Plotted is the difference between the fluorescence values obtained in the absence and presence of an excess (440 nM) of unlabeled EGF versus the amount of FITC-EGF that did not associate with the pellet (free FITC-EGF). The fit of the data to a single class of binding sites indicated that FITC-EGF binds with a dissociation constant of 2.4 ± 0.6 nM, in agreement with competition data. Moreover, quantitation of the growth factor fluorescence showed that the number of FITC-EGF binding sites in the isolated plasma membranes is similar to the number of ^{125}I-EGF binding sites (14 ± 3 and 11 ± 2 nM, respectively) measured in direct binding experiments.

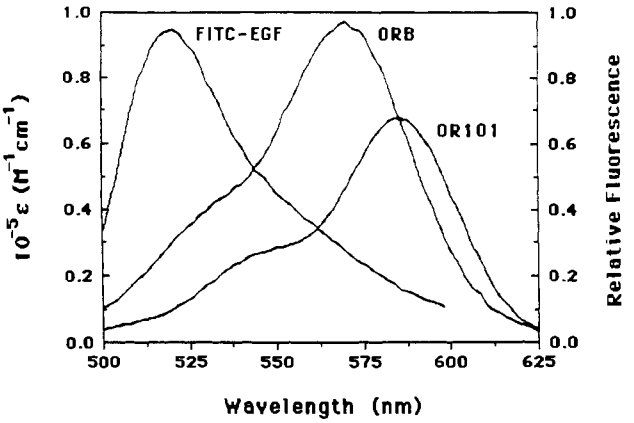

FIGURE 2: Spectral overlap of FITC-EGF emission and the absorption of amphipathic probes inserted into A431 membranes. The corrected emission spectrum of FITC-EGF (ex 460 nm, em 520 nm) is shown with the molar extinction coefficients of the ORB and OR101 probes inserted into A431 membranes.

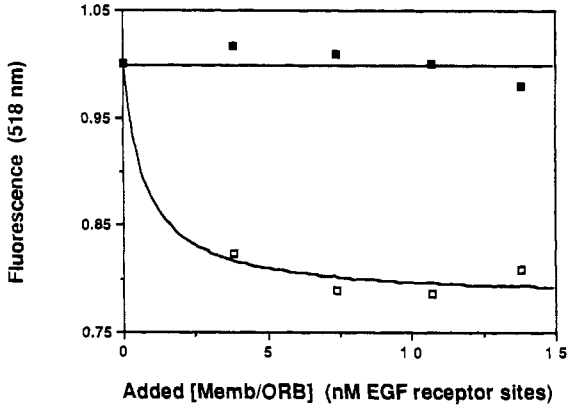

FIGURE 3: Titration of FITC-EGF with ORB-labeled A431 membranes. Membranes were labeled to a high density (~0.9 acceptors/R_0^2) with ORB and used to titrate 5 nM fluorescein-labeled EGF (ex 460 nm, em 518 nm) in the presence (■) and absence (□) of an excess (440 nM) of unlabeled EGF. The amount of membranes added is expressed in terms of the final concentration of ^{125}I-EGF binding sites.

Energy Transfer between FITC-EGF and ORB-Labeled Membranes. Figure 2 shows the fluorescence emission spectrum for FITC-EGF and the absorption spectra for two rhodamine-containing lipid moieties, ORB and OR101. On the basis of the spectral overlap between the fluorescein emission and the rhodamine absorption, R_0 values for the FITC-EGF/ORB and FITC-EGF/OR101 donor/acceptor pairs were calculated to be 55.7 and 49.7 Å, respectively. Thus, these chromophores represent good choices for donor/acceptor pairs in measuring the relative distance of the receptor-bound EGF molecule to the surface of the membrane. Figure 3 shows the results of an experiment in which 5 nM FITC-EGF was titrated with A431 plasma membranes, labeled to a high density (~0.9 acceptors/R_0^2) with ORB, in the presence and absence of an excess of unlabeled EGF. A significant degree of fluorescein quenching occurred upon titration of the labeled growth factor with ORB/membranes. This quenching was blocked in the presence of an excess of unlabeled EGF. Moreover, addition of an excess of unlabeled EGF to the FITC-EGF/labeled membrane complexes relieved the quenching at a rate consistent with the off rate of ^{125}I-EGF interaction with its membrane receptor (not shown). Thus, these results showed that a significant degree of resonance energy transfer occurred between the bound FITC-EGF molecule and chromophoric lipids distributed along the surface of A431 cell plasma membranes. We also found that, even

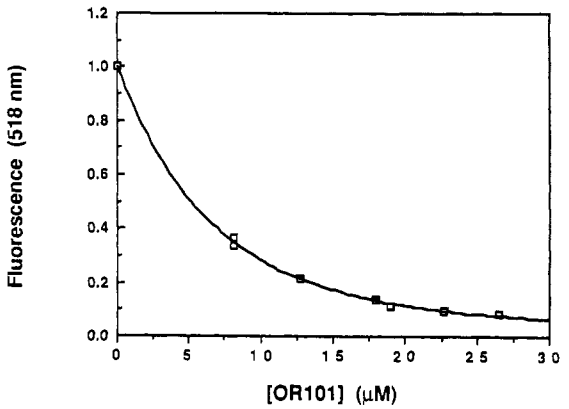

FIGURE 4: Determination of OR101 density in A431 plasma membranes. The density of OR101 in labeled membranes was determined by fitting the quenching of HAF fluorescence by OR101 to eq 1. Depicted is the extent of HAF quenching as a function of the concentration of OR101 contained in each sample. The curve through the data points represents the nonlinear least-squares fit to eq 1.

at high densities of ORB in A431 membranes, the fluorescence of the rhodamine probe did not interfere with the donor FITC-EGF fluorescence, and quenching due to inner filter effects was essentially negligible.

Determination of the Density of Lipophilic Probes in Membranes Isolated from A431 Cells. Various quantities of the amphipathic energy transfer acceptors ORB and OR101 were independently inserted into A431 plasma membrane vesicle bilayers, and the densities of the inserted probes were determined by their ability to quench the fluorescence of [(hexadecyl)amino]fluorescein (HAF), as previously described (Holowka & Baird, 1983). Figure 4 shows a plot of the HAF fluorescence as a function of the concentration of OR101 in the plasma membrane vesicles. A very similar plot was obtained when a 10-fold higher concentration of HAF was employed (data not shown), which indicated that the rhodamine-containing acceptor lipids were randomly distributed along the membrane surface. The data were fit to eq 1 to obtain the parameter P, which allowed the conversion of OR101 concentration to the density of the probe in the plasma membranes (acceptors/R_0^2). Similar plots and fits were constructed for ORB inserted into plasma membrane vesicles. Control experiments indicated that essentially all of the acceptor probe (>98%) remained associated with the A431 membranes throughout the time period of the energy transfer measurements performed for both the density determination and the determination of the distance of closest approach.

Measurement of the Distance of Closest Approach (L). The distance of closest approach, which represents the minimum possible distance between an acceptor chromophore at the surface of the plasma membrane and the fluorescent label on the amino terminus of the growth factor molecule, was determined with the use of Monte Carlo simulations, as described by Snyder and Freire (1982). A titration of acceptor-labeled membranes with FITC-EGF was performed at each acceptor density. For example, Figure 5a shows the FITC-EGF fluorescence at 518 nm as a function of added [FITC-EGF], at various densities of OR101 in the plasma membrane. The data indicated that as the density of OR101 in the plasma membrane increased, there was a corresponding increase in the quenching of the FITC-EGF fluorescence. In all cases, the extent of quenching was corrected for inner filter effects; however, even at the highest acceptor densities employed, the extinction coefficients for the acceptor probe at the excitation and emission wavelengths were sufficiently low such that little inner filter quenching (<2%) should occur.

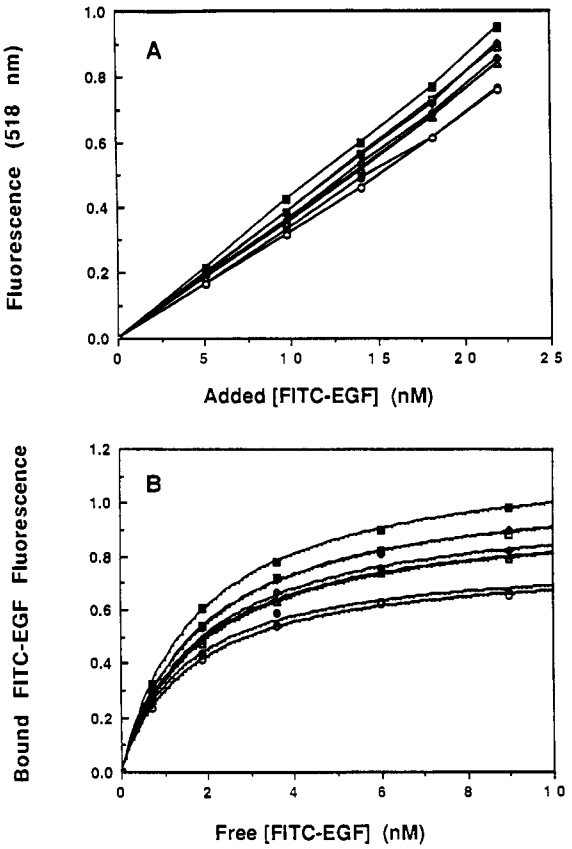

FIGURE 5: FITC-EGF titrations of OR101 labeled membranes. FITC-EGF was titrated into A431 membranes labeled with OR101 at acceptor densities of 0 (■), 0.32 (□, ◆) 0.50 (◇), 0.70 (▲), 0.74 (△), 0.88 (●), and 1.03 (○) acceptors/R_0^2, and the fluorescence (ex 460, em 518) was determined. (A) The fluorescence data (corrected for background and inner filter quenching) are plotted as a function of the total [FITC-EGF] in solution. (B) The same data are replotted after correcting for the contribution of FITC-EGF not bound to EGF receptors, according to eqs 5 and 6.

Because some of the FITC-EGF was free in solution in the experiment depicted in Figure 5a, the fluorescence data had to be corrected for this component of the donor fluorescence which could not contribute to energy transfer. This correction was performed by assuming a single class of sites and a K_d of 2.5 nM for FITC-EGF binding to the EGF receptor, according to eqs 5 and 6. Figure 5b shows a replot of the fluorescence titrations depicted in Figure 5a, corrected for the unbound FITC-EGF. This analysis showed that the fluorescence of the bound FITC-EGF was quenched by 35% at the highest density of acceptor probe. Similar titrations were performed for A431 plasma membranes containing ORB to determine the dependence of donor FITC-EGF fluorescence on the density of this probe.

Five concentrations of FITC-EGF were employed in the titrations described above, which in turn yielded five determinations of resonance energy transfer for each density of the acceptor probes. The averages of these determinations, expressed as Q_{DA}/Q_D, were plotted versus the acceptor probe densities for the two acceptor probes employed in this study. Figure 6 shows these energy transfer data plotted over the theoretical curves for energy transfer between a donor and a plane of acceptors, for L/R_0 ratios ranging from 1.2 to 1.5. The energy transfer data were fit as described under Experimental Procedures, and the fits were interpolated to estimate the L/R_0 ratios for each acceptor probe. The ratios were multiplied by the known R_0 values for energy transfer between FITC-EGF and the two acceptor probes to yield the distances

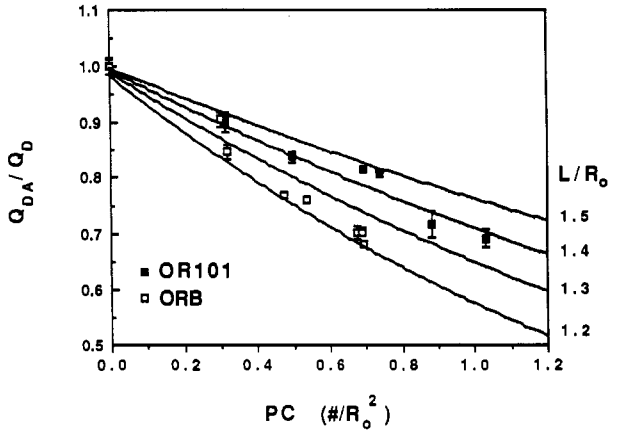

FIGURE 6: Energy transfer between receptor-bound FITC-EGF and amphipathic acceptor probes at the membrane surface. The efficiency of energy transfer, expressed as the ratio of the donor quantum yield in the presence (Q_{DA}) and absence (Q_D) of acceptor, is plotted as a function of the density of acceptor in the plasma membrane, for the acceptors ORB (□) and OR101 (■). The curves represent the single-exponential fits of the theoretical quenching values obtained from eq 7 for L/R_0 values ranging from 1.2 to 1.5, as indicated. Error bars represent the standard error of the calculated energy transfer of receptor-bound FITC-EGF. On the basis of the R_0 values of 55.7 Å for FITC-EGF/ORB and 49.7 Å for FITC-EGF/OR101, we calculate distances of closest approach of 66 ± 1 and 68 ± 1 Å, respectively, for the two acceptor probes.

Table I: Spectral Parameters of Membrane-Bound Donor–Acceptor Pairs

donor	Q_D[a]	A_D[b]	acceptor	A_A[c]	R_0[d] (Å)	L (Å)
FITC-EGF	0.48 ± 0.02	0.18	ORB	0.14	55.7	66 ± 1
FITC-EGF	0.48 ± 0.02	0.18	OR101	0.13	49.7	68 ● 1

[a] The quantum yield of receptor-bound FITC-EGF was measured under conditions that correct for the polarizing effects of the instrumentation. [b] The anisotropy of FITC-EGF free in solution is 0.09. [c] Measured at a probe density of ~3.5×10^{-5}/Å^2. [d] A value of $^2/_3$ was assumed for κ^2; see Discussion.

of closest approach, which were 66 ± 1 Å and 68 ± 1 Å for ORB and OR101, respectively. These data are summarized in Table I.

We have demonstrated previously that the binding of divalent metal ions such as Mg^{2+} and Mn^{2+} to the tyrosine kinase domain of the EGF receptor induces a conformational change within that domain (Koland & Cerione, 1990) that concomitantly activates the receptor kinase activity and aggregates receptors. Therefore, we wanted to determine whether or not metal-induced conformational changes and receptor aggregation could be visualized as a change in the distance of closest approach between the receptor-bound growth factor and lipids in the plasma membrane. To address this question, isolated A431 membranes were labeled to a high density (~0.9 acceptors/R_0^2) with ORB, and energy transfer was measured between receptor-bound FITC-EGF and the acceptor probes within the plasma membranes (data not shown). $MnCl_2$ was added to these membranes (to a final concentration of 5 mM), followed by the addition of 1 mM ATP. No significant change in the level of energy transfer was observed upon the addition of either of these agents, suggesting that events occurring on the cytoplasmic domain of the receptor that stimulate receptor aggregation and autophosphorylation do not result in a significant transverse displacement of the EGF binding domain with respect to the plasma membrane.

Discussion

While the solution structure of murine epidermal growth factor has been solved by two-dimensional NMR (Montelione

et al., 1986, 1987), very little is known about the structure of the receptor for EGF or how this receptor serves to transduce the mitogenic signal across the plasma membrane. We have begun to use fluorescence approaches to study the structure of the EGF receptor with the ultimate aim of characterizing the conformational changes within this molecule that serve in transmembrane signaling.

In the present study, we have used resonance energy transfer to determine that the distance of closest approach between a fluorescent probe on the amino terminus of EGF bound to its receptor and amphipathic probes inserted into isolated plasma membranes from A431 epidermoid carcinoma cells is about 67 Å. We have previously demonstrated that the FITC-EGF-bound receptor is predominantly in a nonaggregated form under the conditions employed in these experiments (Carraway et al., 1989). Because the monomeric EGF receptor appears to contain a very thin membrane-spanning region (a single α-helix ~4–6 Å in diameter), it is likely that the distance of closest approach measured by energy transfer in these studies represents the actual distance between the amino terminus of the growth factor molecule and the surface of the plasma membrane. It is possible that the transmembrane region of the receptor has immobilized lipids associated with it that would not readily exchange with the acceptor lipids inserted into the bilayer. This would lead to an overestimation of the distance of the amino terminus of EGF above the bilayer. However, if it is assumed that the radius of a phospholipid is 4.2 Å (Fung & Stryer, 1978), then it may be determined from geometrical considerations that a layer of phospholipid around the receptor transmembrane helix results in a difference of <10% in our estimate of the distance between the growth factor and the plasma membrane.

The estimation of the distance of closest approach rested on the assumption that the value for κ^2, a parameter characterizing the relative orientations of the donor and acceptor transition dipoles (eq 4), was $^2/_3$. This value represents the situation in which the donor and acceptor probes rotate rapidly relative to the lifetime of donor fluorescence. However, the anisotropy values for the donor and acceptor probes indicate that there is some limitation to the degree of rotational freedom of both the donor and acceptor moieties. On the basis of these anisotropy data, the maximum and minimum values of κ^2 may be estimated (Dale et al., 1979) and the range of R_0 values determined for each donor/acceptor pair. This analysis suggests that the uncertainty in the value of κ^2 introduces an error of ±12% in our distance determination. Another potential source of uncertainty concerns the localization of acceptor lipids in the plasma membrane. Our calculations of acceptor density are based on the assumption that energy transfer occurs only between donor HAF and acceptor probes situated on the same side of the plasma membrane. However, the A431 plasma membranes employed in these studies were permeant to proteins as large as 60 kD. Hence, we predict that both the donor and acceptor amphipathic probes actually distributed evenly between the inner and outer leaflets of the membrane and that some energy transfer occurred between donors and acceptors on opposite sides of the membrane. If it is assumed that the thickness of the plasma membrane is 60 Å, it may be calculated that we overestimated the acceptor densities by ~8% and thus overestimated the distance of closest approach by 1–2 Å.

On the basis of sequence alignment studies, Bajaj et al. (1987) have proposed structures for the extracellular domains of the EGF receptor and other receptor tyrosine kinases. For the case of the EGF receptor, the extracellular domain was suggested to be composed of two large homologous subdomains, each of which is followed in sequence by three cysteine-rich regions. It was further hypothesized that the EGF receptor extracellular domain is organized as a pseudosymmetrical dimer in solution, with the two large subdomains far from the plasma membrane and the cysteine-rich subdomains close to the membrane. Chemical cross-linking experiments (Lax et al., 1988; Wu et al., 1990) as well as studies with chimeric human/chicken EGF receptors and human receptors truncated in their extracellular domains (Lax et al., 1989, 1990) have suggested that at least one of these large domains is responsible for binding EGF with high affinity. This in turn would suggest that the EGF binding site on the receptor is some distance from the plasma membrane. Our energy transfer data appears to confirm such a prediction. On the basis of two-dimensional NMR studies (Montelione et al., 1986, 1987), it is known that the distance from the amino terminus of EGF to the center of the molecule is ~15 Å. This, together with our energy transfer measurements, suggests that the EGF molecule binds to a site on the receptor that is at least 52 Å away and perhaps as far as 82 Å away from the plasma membrane.

One of the motivating factors in applying fluorescence techniques to the study of growth factor receptors is the potential utilization of these techniques to detect conformational changes within receptor proteins. Using resonance energy transfer between donor- and acceptor-labeled growth factor molecules, we have previously demonstrated that metal ion activators of the EGF receptor tyrosine kinase activity (Mg^{2+} and Mn^{2+}) promoted the aggregation of receptors in isolated A431 cell membranes (Carraway et al., 1989). In an effort to begin to correlate conformational changes within the EGF receptor with the activation of its tyrosine kinase activity, we examined the effect of divalent metal ions on the extent of energy transfer between the receptor-bound FITC-EGF molecules and ORB molecules distributed within plasma membranes isolated from A431 cells. We found that the addition of the divalent metal ion activators had no effect on the distance measured between the labeled growth factor and the membrane surface. Similarly, the addition of sufficient ATP to insure full EGF receptor autophosphorylation did not alter these distance measurements. These results suggest that divalent metal ion interactions with the cytoplasmic domain of the receptor, which are required for both the activation of the tyrosine kinase activity and for full aggregation of EGF receptor molecules, do not cause a significant transverse displacement of the growth factor binding domain with respect to the plasma membrane. However, it is possible that such a transverse displacement is elicited by the initial binding of the labeled growth factor to its binding site within the extracellular domain of the receptor. Future studies using energy transfer and other fluorescence techniques will focus on characterizing the conformational changes within both the extracellular and cytoplasmic domains of the EGF receptor molecule that occur upon activation with the growth factor or with divalent metal cations.

Registry No. EGF, 62229-50-9; Mn^{2+}, 7439-96-5; EGF receptor tyrosine kinase, 79079-06-4.

References

Bajaj, M., Waterfield, M. D., Schlessinger, J., Taylor, W. R., & Blundell, T. (1987) *Biochim. Biophys. Acta 916*, 220–226.

Boni-Schnetzler, M., & Pilch, P. F. (1987) *Proc. Natl. Acad. Sci. U.S.A. 84*, 7832–7836.

Cantley, L. C., Jr., & Hammes, G. G. (1975) *Biochemistry 14*, 2976–2981.
Carpenter, G. (1987) *Annu. Rev. Biochem. 48*, 193–216.
Carraway, K. L., Koland, J. G., & Cerione, R. A. (1989) *J. Biol. Chem. 264*, 8699–8707.
Chen, W. S., Lazar, C. S., Poenie, M., Tsien, R. Y., Gill, G. N., & Rosenfeld, M. G. (1987) *Nature 328*, 820–823.
Dale, R. E., Eisinger, J., & Blumberg, W. E. (1979) *Biophys. J. 26*, 161–194.
Forster, T. (1959) *Discuss. Faraday Soc. 27*, 7–17.
Fung, B. K.-K., & Stryer, L. (1978) *Biochemistry 17*, 5241–5248.
Greenfield, C., Hiles, I., Waterfield, M. D., Federwisch, M., Wollmer, A., Blundell, T. L., & McDonald, N. (1989) *EMBO J. 8*, 4115–4123.
Holowka, D., & Baird, B. (1983) *Biochemistry 22*, 3466–3474.
Honnegger, A., Dull, T. J., Bellot, F., Van Obberghen, E., Szapary, D., Schmidt, A., Ullrich, A., & Schlessinger, J. (1988) *EMBO J. 7*, 3045–3052.
Hunter, T., & Cooper, J. A. (1985) *Annu. Rev. Biochem. 54*, 897–930.
Koland, J. G., & Cerione, R. A. (1988) *J. Biol. Chem. 263*, 2230–2237.
Koland, J. G., & Cerione, R. A. (1990) *Biochim. Biophys. Acta* (in press).
Lax, I., Burgess, W. H., Bellot, F., Ullrich, A., Schlessinger, J., & Givol, D. (1988) *Mol. Cell. Biol. 8*, 1831–1834.
Lax, I., Bellot, F., Howk, R., Ullrich, A., Givol, D., & Schlessinger, J. (1989) *EMBO J. 8*, 421–427.
Lax, I., Bellot, F., Honegger, A. M., Schmidt, A., Ullrich, A., Givol, D., & Schlessinger, J. (1990) *Cell Regul. 1*, 173–188.
Montelione, G. T., Wuthrich, K., Nice, E. C., Burgess, A. W., & Scheraga, H. A. (1986) *Proc. Natl. Acad. Sci. U.S.A. 83*, 8594–8598.
Montelione, G. T., Wuthrich, K., Nice, E. C., Burgess, A. W., & Scheraga, H. A. (1987) *Proc. Natl. Acad. Sci. U.S.A. 84*, 5226–5230.
Schlessinger, J. (1986) *J. Cell Biol. 103*, 2067–2072.
Snyder, B., & Freire, E. (1982) *Biophys. J. 40*, 137–148.
Thom, D., Powell, A. J., Lloyd, C. W., & Rees, D. A. (1987) *Biochem. J. 168*, 187–194.
Ullrich, A., Coussens, L., Hayflick, J. S., Dull, T. J., Gray, A., Tam, A. W., Lee, J., Yarden, Y., Libermann, T. A., Schlessinger, J., Downward, J., Mayes, E. L. V., Whittle, N., Waterfield, M. D., & Seeburg, P. H. (1984) *Nature 309*, 418–425.
Weber, G., & Teale, F. W. J. (1957) *Trans. Faraday Soc. 53*, 645–655.
Wolber, P. K., & Hudson, B. S. (1979) *Biophys. J. 28*, 197–210.
Wu, D., Wang, L., Chi, Y., Sato, G. H., & Sato, J. D. (1990) *Proc. Natl. Acad. Sci. U.S.A. 87*, 3151–3155.
Yarden, Y., & Schlessinger, J. (1987a) *Biochemistry 26*, 1434–1442.
Yarden, Y., & Schlessinger, J. (1987b) *Biochemistry 26*, 1443–1451.

Enzymic Synthesis of Oligonucleotides Containing Methylphosphonate Internucleotide Linkages

Hirotaka Higuchi,[‡] Tohru Endo,[‡] and Akira Kaji*[,§]

Research Institute for Molecular Genetics, Tsumura & Company, 3586 Yoshiwara, Ami, Ibaraki, Japan, and Department of Microbiology, School of Medicine, University of Pennsylvania, Philadelphia, Pennsylvania 19104-6076

Received February 14, 1990; Revised Manuscript Received May 29, 1990

ABSTRACT: Thymidine 5′-*O*-(pyrophosphoryl methylphosphonate) (dTTPαCH3) has been chemically synthesized by condensation of thymidine 5′-*O*-(methylphosphonate) with pyrophosphate. This novel nucleotide, which contained an α-phosphorus atom as methylphosphonate, was used as a substrate of terminal deoxynucleotidyltransferase (TDTase) in the presence of oligonucleotide (5′-GCTGTATCGTCA-AGGCACTC-3′) as an initiator. The reaction products were separated into two components by reverse-phase high-performance liquid chromatography (RP-HPLC). These products were, after purification, digested with nuclease P1 and alkaline phosphatase followed by separation of digested products by RP-HPLC. The result showed the presence of one of the isomers of 2′-deoxycytidyl-3′-methylphosphonyl-5′-thymidine (dCpCH3T) and 2′-deoxycytidyl-3′-methylphosphonyl-5′-thymidyl-3′-methylphosphonyl-5′-thymidine (dCpCH3TpCH3T), respectively. Fast atom bombardment mass spectrometry of these products further supported identification of the dinucleotide and the trinucleotide. These results indicated that dTTPαCH3 was used as a substrate of TDTase, resulting in methylphosphonate linkages. Produced oligomers were resistant to hydrolysis by snake venom phosphodiesterase I.

Oligonucleoside methylphosphonates, backbone-modified oligomers containing uncharged methylphosphonate internucleotide linkages, have been chemically synthesized and used by several laboratories. For example, owing to their stability to nucleases and permeability into mammalian cells (Agarwal & Riftina, 1979; Miller et al., 1981), these analogues have been used as antisense oligonucleotides to inhibit replication of a number of DNA or RNA viruses including human immunodeficiency virus (HIV)[1] (Miller et al., 1985; Smith et

* Author to whom correspondence should be addressed.
‡ Research Institute for Molecular Genetics, Tsumura & Co.
§ University of Pennsylvania.

0006-2960/90/0429-8747$02.50/0